

Received: 2017.10.10
Accepted: 2018.01.10
Published: 2018.02.07

Silencing Ras-Related C3 Botulinum Toxin Substrate 1 Inhibits Growth and Migration of Hypopharyngeal Squamous Cell Carcinoma via the P38 Mitogen-Activated Protein Kinase Signaling Pathway

Authors' Contribution:
Study Design A
Data Collection B
Statistical Analysis C
Data Interpretation D
Manuscript Preparation E
Literature Search F
Funds Collection G

AEF 1 **Huijuan Cheng**
ABCDE 2 **Weiwei Wang**
BCDE 2 **Guangke Wang**
BCDE 3 **Anran Wang**
BCD 1 **Linfang Du**
AEF 1 **Weihua Lou**

1 Department of Otolaryngology, Head and Neck Surgery, The First Affiliated Hospital of Zhengzhou University, Zhengzhou, Henan, P.R. China
2 Department of Otolaryngology, Henan Provincial People's Hospital, Zhengzhou, Henan, P.R. China
3 Department of Neurosurgery, The First Affiliated Hospital of Zhengzhou University, Zhengzhou, Henan, P.R. China

Corresponding Author: Weihua Lou, e-mail: louweihuazzu@126.com
Source of support: Departmental sources

Background: Ras-related C3 botulinum toxin substrate 1 (Rac1) is implicated in a variety of cellular functions and is related to tumor growth and metastasis. This study aimed to explore the role of Rac1 in hypopharyngeal squamous cell carcinoma (HSCC).

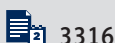
Material/Methods: The Rac1 expression in HSCC tissues was determined by quantitative real-time polymerase chain reaction and Western blot analysis. The level of Rac1 in HSCC cells was downregulated by a Rac1-specific shRNA. Then, the growth and metastasis of HSCC cells were assessed *in vitro* by 3-(4,5-dimethyl-2-thiazolyl)-2,5-diphenyl-2-H-tetrazolium bromide assay, flow cytometry, Hoechst staining, and Transwell assay. Moreover, cells transfected with Rac1 shRNA or negative control were injected subcutaneously into the right axilla of mice, and then the effects of Rac1 silencing on the growth of HSCC were also explored *in vivo*. Additionally, activation of the P38 mitogen-activated protein kinase (MAPK) signaling pathway was assessed by Western blot.

Results: Rac1 was highly expressed in HSCC tissues. Silencing Rac1 inhibited the proliferation and cell cycle progress of HSCC cells, and induced their apoptosis. Rac1 silencing also suppressed the migration and invasion of HSCC cells. *In vivo* study showed that silencing Rac1 suppressed the growth of tumor bodies. Moreover, the P38 MAPK signaling pathway was implicated in the tumor-suppressing effect of Rac1 silencing *in vitro* and *in vivo*.

Conclusions: Silencing Rac1 suppressed the growth and migration of HSCC through the P38 MAPK signaling pathway. Due to its contribution in HSCC, Rac1 has the potential to become a promising antitumor therapeutic target for HSCC.

MeSH Keywords: **Growth • Hypopharyngeal Neoplasms • Migration • p38 Mitogen-Activated Protein Kinases • Ras-Related C3 Botulinum Toxin Substrate 1**

Full-text PDF: <https://www.medscimonit.com/abstract/index/idArt/907468>



3316



3



10



43



Background

Hypopharyngeal squamous cell carcinoma (HSCC) is a type of aggressive head and neck squamous cell carcinoma originating from hypopharynx mucosa. Patients with HSCC are usually diagnosed at its advanced stages with poor prognosis [1,2]. In recent years, a comprehensive treatment strategy for HSCC is combining surgery, chemotherapy, and radiotherapy [3]. Despite of the improvements in treatment strategies, patients with HSCC show high risks of local recurrence or distant metastases, with a 5-year survival rate of approximately 25–40% [4].

Ras-related C3 botulinum toxin substrate 1 (Rac1) is one of the Rho family small GTPases. It cycles between the active form (guanosine triphosphate (GTP)-bound) and inactive form (guanosine diphosphate (GDP)-bound). Rac1 is activated by guanine nucleotide exchange factors through accelerating the exchange of GDP to GTP, and inactivated by GTPase activating proteins through promoting GTP hydrolysis. In its activated form, Rac1 interacts with its effectors to regulate multiple downstream signals [5]. Rac1 is implicated in a variety of cellular functions, such as cytoskeleton reorganization, gene transcription, cellular motility, and cell division and survival [6–9].

Elevated levels of Rac1 are found in many kinds of cancers, and Rac1 is involved in the proliferation, apoptosis, migration, invasion, and angiogenesis of cancer cells [10–14]. However, the role of Rac1 in HSCC remains unclear. In our present study, we explored the role of Rac1 in HSCC. The results of our study reveal that Rac1 may contribute to the growth and metastasis of HSCC.

Material and Methods

Clinical specimens

HSCC tissues and pericarcinomatous tissues were collected from 20 HSCC patients at the First Affiliated Hospital of Zhengzhou University (Zhengzhou, China) during November 2016 to March 2017. None of these patients had previously received chemotherapy or radiotherapy. Written informed consents were signed by all patients.

Cells

FaDu cells were obtained from ZhongQiaoXinZhou Biotechnology Co., LTD (Shanghai, China). FaDu cells were grown in Minimum Essential Media (Gibco, Grand Island, NY, USA) with 10% fetal bovine serum (FBS, Hyclone, Logan, UT, USA) and cultured in a cell incubator at 37°C with 5% CO₂.

Transfection

Cells were seeded in a 6-well plate (3×10⁵ cells/well). Twenty-four hours later, plasmids containing Rac1 shRNA or negative control (Table 1) were transfected into cells using Lipofectamine 2000 Reagent (Invitrogen, Carlsbad, CA, USA). Thereafter, the cells were selected using G418 (Invitrogen). Cells stably transfected with Rac1 shRNA and negative control were marked as Rac1 shRNA and negative control, respectively. Cells without transfection were marked as parental.

Quantitative real-time polymerase chain reaction (qRT-PCR)

Total ribonucleic acid (RNA) was extracted with a High-purity Total RNA Fast Extraction Kit (BioTeke, Beijing, China) and reversely transcribed to complementary deoxyribonucleic acid (cDNA). The messenger RNA (mRNA) level of Rac1 was detected by qRT-PCR using primers listed in Table 2. The mRNA level in clinical specimens was calculated using 2^{-ΔCt} method and the mRNA level in cells was calculated using 2^{-ΔΔCt} method.

Western blot

Proteins were extracted using radioimmunoprecipitation assay lysis buffer with 1% phenyl-methane-sulfonyl fluoride (PMSF) (Beyotime, Shanghai, China). The protein concentration was measured with a Bicinchoninic Acid Protein Assay Kit (Beyotime). Then, equal proteins from each group were separated by sodium dodecyl sulfate-polyacrylamide gel electrophoresis (SDS-PAGE), followed by transfer onto polyvinylidene fluoride membranes (Millipore, Bedford, MA, USA). The membranes were blocked with 5% skim milk or 1% bovine serum albumin, and then incubated with Rac1 antibody, glyceraldehyde-3-phosphate dehydrogenase (GAPDH) antibody (1: 1000; Proteintech, Wuhan, China), Cyclin D1 antibody (1: 1000;

Table 1. Sequences of Rac1 shRNA and its negative control.

Name	Sense	Antisense
Rac1 shRNA	5'-GATCCCGGATACAGCTGGACAAGAATT CAAGAGATTCTGTCCAGCTGTATCCTTTTT-3'	5'-AGCTAAAAGGATACAGCTGGACAAGA ATCTCTGAATTCTGTCCAGCTGTATCCGGG-3'
Negative control	5'-GATCCCCTTCTCCGAACGTGTACAGTTTC AAGAGAACGTGACACGTTTCGAGAATTTTT-3'	5'-AGCTAAAATTCTCCGAACGTGTACAGTTTC CTTGAAACGTGACACGTTTCGAGAAGGG-3'

Table 2. Sequences of primers for quantitative real-time PCR.

Gene name	Forward primer	Reverse primer
Rac1	5'-CGAGAACTGAAGGAGAAGAAGC-3'	5'-AAGGGACAGGACCAAGAACGAG-3'
GAPDH	5'-GAAGGTCGGAGTCAACGGAT-3'	5'-CCTGGAAGATGGTATGGGAT-3'

BOSTER, Wuhan, China), Cyclin E antibody, Cyclin B antibody (1: 500; Bioss, Beijing, China), metal matrix proteinase (MMP)-2 antibody, MMP-9 antibody, B cell lymphoma-2 (Bcl-2) antibody, Bcl-2-associated X protein (Bax) antibody, phosphorylated-MAP kinase (p-MKK3) antibody (1: 500; Sangon Biotech, Shanghai, China), caspase-3 antibody, caspase-9 antibody, poly ADP-ribose polymerase (PARP) antibody (1: 1000; Cell Signaling Technology, Beverly, MA, USA), p38 mitogen-activated protein kinase (MAPK) antibody, p-p38 MAPK antibody (1: 500; KeyGen, Nanjing, China), or MKK3 antibody (1: 300; BOSTER) overnight at 4°C. The membranes were rinsed in Tris-buffered saline with tween (TBST) and then incubated with horseradish peroxidase-conjugated secondary antibodies (1: 5000; Beyotime) for 45 min at 37°C. Then, the membranes were rinsed in TBST and visualized with an Enhanced Chemiluminescence Kit (Beyotime).

3-(4,5-dimethyl-2-thiazolyl)-2,5-diphenyl-2-H-tetrazolium bromide (MTT) assay

Cells were seeded in 96-well plates with 4×10^3 cells per well and cultured for 0 h, 24 h, 48 h, 72 h, and 96 h. After adding MTT (Sigma, St. Louis, MO, USA) into each well and incubating for 4 h at 37°C, 150 μ l of dimethyl sulfoxide (Sigma) was added to dissolve the crystals formed. Absorbance at 570 nm was measured with a microplate reader.

Cell cycle assay

Flow cytometry was used to analyze the cell cycle with a Cell Cycle Detection Kit (Beyotime). Cells were collected, rinsed in PBS, and fixed in ice-cold 70% ethanol at 4°C for 2 h. The cells were then rinsed in phosphate-buffered saline (PBS) and resuspended in 500 μ l of staining buffer. Then, 25 μ l of propidium iodide and 10 μ l of RNase A were added into cells and incubated for 30 min at 37°C. Cells were then analyzed with a flow cytometer (BD, Franklin Lakes, NJ, USA).

Transwell assay

To assess the migration capability, cells were made into single-cell suspensions and seeded into Transwell inserts (Corning, Tewksbury, MA, USA) in a 24-well plate (5×10^3 cells in 200 μ l of serum-free cell medium). To the lower chambers, we added 800 μ l of cell medium containing 30% FBS. Then, the cells were incubated in a cell incubator for 24 h, rinsed in PBS, fixed in 4% paraformaldehyde, and stained in crystal violet dye (Amresco,

Solon, USA). The cells were observed and photographed with a microscope at 200 \times magnification. The number of migratory cells was calculated.

To assess the invasion capability, 200 μ l of single-cell-suspensions (1×10^4 cells in serum-free cell medium) were added into the Transwell inserts pre-coated with Matrigel (BD), and 800 μ l of cell medium containing 30% FBS was added into the lower chambers. After invasion for 24 h, the cells were stained with crystal violet dye and images were captured as described above.

Gelatin zymography

Proteins were extracted using ice-cold PBS with 1% PMSF. Following measurement of protein concentration, equal proteins from each group was injected into SDS-PAGE containing 10 mg/ml gelatin. After electrophoresis, the gel was rinsed in elution buffer and washing buffer, and then incubated in incubation buffer at 37°C for 40 h. Thereafter, the gel was kept in staining buffer for 3 h, followed by destaining buffer A for 0.5 h, destaining buffer B for 1 h, and destaining buffer C for 2 h. Images of gel were captured using a Gel Imaging System (Liuyi, Beijing, China).

Hoechst staining

Cells were seeded onto coverslips in 12 well plates (3×10^4 cells/well). After culture for 24 h, the cells were rinsed in PBS and fixed in 4% paraformaldehyde. Then, the cells were rinsed and stained in Hoechst dye (Beyotime). Images were captured with a fluorescence microscope at 400 \times magnification.

Animal experimental protocol

Healthy BALB/c nude mice (female, 6-weeks-old, weighing 16–18 g) were obtained from Huafukang Bioscience Co., Inc (Beijing, China). Mice were fed in a controlled environment ($27 \pm 1^\circ\text{C}$, $50 \pm 10\%$ humidity, 12 h/12 h light/dark cycles) and had free access to food and water. Mice were randomly divided into 3 groups (parental, negative control, and Rac1 shRNA) with 6 mice in each group. Rac1 shRNA cells, negative control cells, and parental cells (1×10^7 cells in 0.1 ml of serum-free medium) were injected subcutaneously into the right axilla of mice in the Rac1 shRNA group, negative control group, and parental group, respectively. Thereafter, mice and tumor bodies were observed every day. The longest diameters and

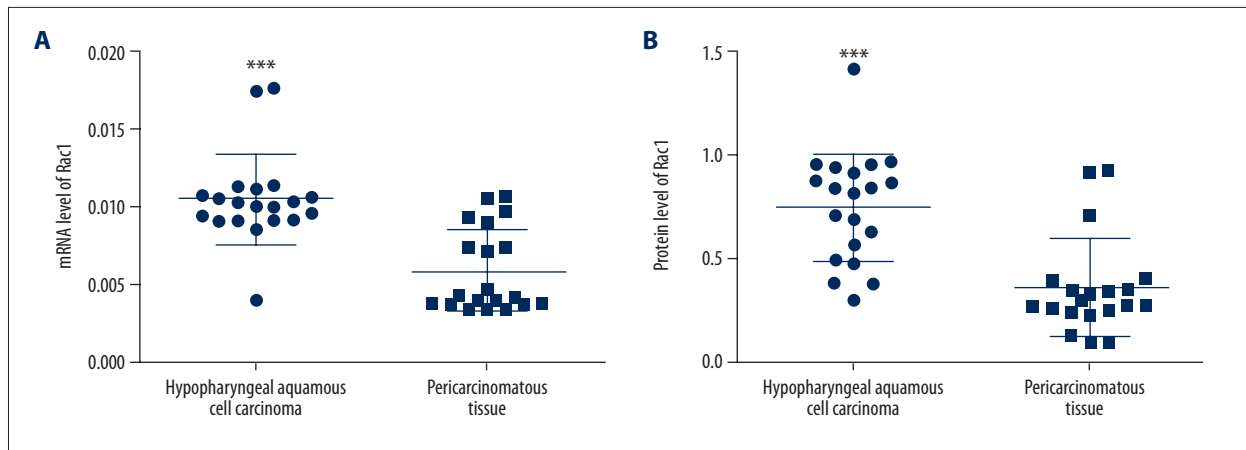


Figure 1. Rac1 is up-regulated in HSCC. (A) mRNA level of Rac1 in HSCC tissues and pericarcinomatous tissues was detected by qRT-PCR. The results were calculated using $2^{-\Delta\Delta Ct}$ method. (B) Protein level of Rac1 in HSCC tissues and pericarcinomatous tissues was detected by Western blot. The results are presented as mean \pm SD. *** $P < 0.001$.

shortest diameters of tumor bodies in each group were recorded every 3 days. Thirty days later, the mice were killed and the tumor bodies were obtained. Images of mice and tumor bodies were captured and the weights of tumor bodies were recorded. This study was performed according to the Guide for Care and Use of Laboratory Animals and was approved by the Ethics Committee of the First Affiliated Hospital of Zhengzhou University.

Hematoxylin-eosin (HE) staining

The tumor bodies were obtained and fixed in 4% paraformaldehyde. Then, the tumor bodies were dehydrated in graded ethanol, embedded in paraffin, and cut into 5- μ m sections. Thereafter, the sections were subjected to routine HE staining. Images were captured at 200 \times magnification.

Terminal deoxynucleotidyl transferase-mediated dUTP nick-end labeling (TUNEL) assay

Apoptosis in the tumor bodies were detected by TUNEL assay with an In Situ Cell Death Detection Kit (Roche, Penzberg, Germany). The tumor bodies were collected, embedded in paraffin, and cut into 5- μ m sections. Then, the sections were deparaffinated in xylene, rehydrated in graded ethanol, permeabilized in 0.1% Triton X-100, and blocked with 3% H_2O_2 . After rinsing in PBS, the sections were incubated with TUNEL reaction solution for 60 min at 37 $^{\circ}$ C in the dark. The sections were rinsed in PBS and incubated with Converter-POD at 37 $^{\circ}$ C for 30 min. After rinsing, the sections were developed with DAB Color-Substrate Solution (Solarbio) and counterstained with hematoxylin. The sections were observed and photographed at 400 \times magnification.

Statistical analysis

The results are shown as mean \pm standard deviation (SD). Analysis of data was performed using Student's *t* test or one-way analysis of variance followed by the Bonferroni multiple comparison test. $P < 0.05$ was considered as significant.

Results

Rac1 is highly expressed in HSCC tissues

To assess the Rac1 level in HSCC, the mRNA and protein levels of Rac1 in HSCC tissues and pericarcinomatous tissues were measured. The mRNA level of Rac1 in HSCC tissues was much higher than that in pericarcinomatous tissues (Figure 1A). Similarly, the Rac1 protein level in HSCC tissues was higher than that in pericarcinomatous tissues (Figure 1B). These results reveal that Rac1 is highly expressed in HSCC.

Silencing Rac1 inhibits the growth of HSCC cells *in vitro*

To explore the role of Rac1 in HSCC, a Rac1-specific shRNA was used to down-regulate the Rac1 level. Prior to this study, the efficiency of Rac1 shRNA was verified. Cells transfected with Rac1 shRNA showed a lower Rac1 mRNA level and lower Rac1 protein level (Figure 2) compared with the negative control group. Then, the proliferation of FaDu cells was assessed by MTT assay. Cells transfected with Rac1 shRNA showed a slower proliferation compared with the negative control group (Figure 3A), indicating a growth-inhibition role of Rac1 silencing in FaDu cells.

The cell cycle is one of the important events in cell growth. In our study, the effects of Rac1 silencing on the cell cycle of FaDu cells were assessed by flow cytometry. After silencing

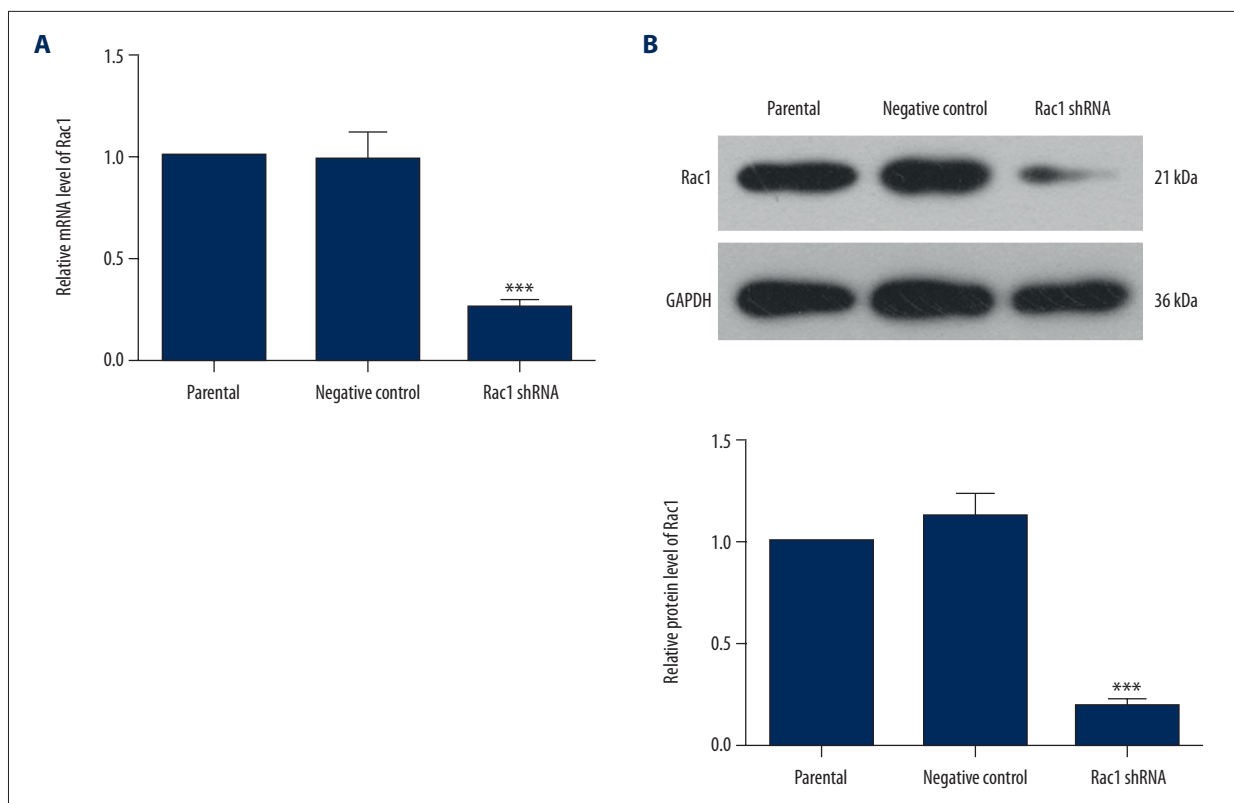


Figure 2. Rac1 shRNA decreases the level of Rac1. **(A)** mRNA level of Rac1 in each group was measured using quantitative real-time PCR. The relative mRNA level of Rac1 was calculated using $2^{-\Delta\Delta Ct}$ method. **(B)** The protein level of Rac1 was detected by Western blot with GAPDH as the internal reference. All experiments were repeated 3 times. The results are presented as mean \pm SD. *** $P < 0.001$ compared with the negative control group.

Rac1, the ratio of cells in G1 phase was increased significantly, whereas the ratios of cells in S phase and G2/M phase were decreased (Figure 3B, Table 3). The protein levels of cyclins were also detected by Western blot. Cells in the Rac1 shRNA group showed lower cyclinB (Figure 3C), cyclinD1 (Figure 3D), and cyclinE (Figure 3E) levels. These results demonstrate that Rac1 silencing suppresses the cell cycle of FaDu cells.

Silencing Rac1 induces apoptosis in FaDu cells

The effects of Rac1 silencing on apoptosis were explored in our study. The results of apoptosis assessed by Hoechst staining showed that there were more chromatin condensations in Rac1 shRNA cells (Figure 4). The protein levels of caspase-3, caspase-9, PARP, Bax, and Bcl-2, which have close relationships with apoptosis, were also detected in our study. After silencing Rac1, the levels of pro-caspase-3, pro-caspase-9, and PARP were decreased significantly, whereas the cleaved caspase-3, cleaved caspase-9, and cleaved PARP levels were increased (Figure 5A–5F). Rac1 shRNA cells also showed a higher Bax level and a lower Bcl-2 level (Figure 5G–5J). These results show that Rac1 silencing induces apoptosis in FaDu cells.

Silencing Rac1 suppresses the migration and invasion of FaDu cells

The effects of Rac1 shRNA on migration and invasion of FaDu cells were assessed by Transwell assay. The Rac1 shRNA group showed fewer migratory cells (Figure 6A) and fewer invasive cells (Figure 6B). Moreover, the expression and activities of MMP-2 and MMP-9, which have close relationships with migration and invasion of cells, were detected. The results of Western blot showed that cells in the Rac1 shRNA group showed lower expression levels of MMP-2 and MMP-9 (Figure 7A–7D). The results of gelatin zymography assay also showed lower MMP-2 and MMP-9 activities in the Rac1 shRNA group (Figure 7E, 7F). These results demonstrate that Rac1 silencing suppresses the migration and invasion of FaDu cells.

Rac1 silencing inhibits the activation of P38 MAPK signaling pathway

The activation of P38 MAPK signaling after Rac1 silencing was explored in our study. There was no significant change in the protein level of MKK3. However, the phosphorylation level of MKK3 was decreased significantly (Figure 8A, 8B). The

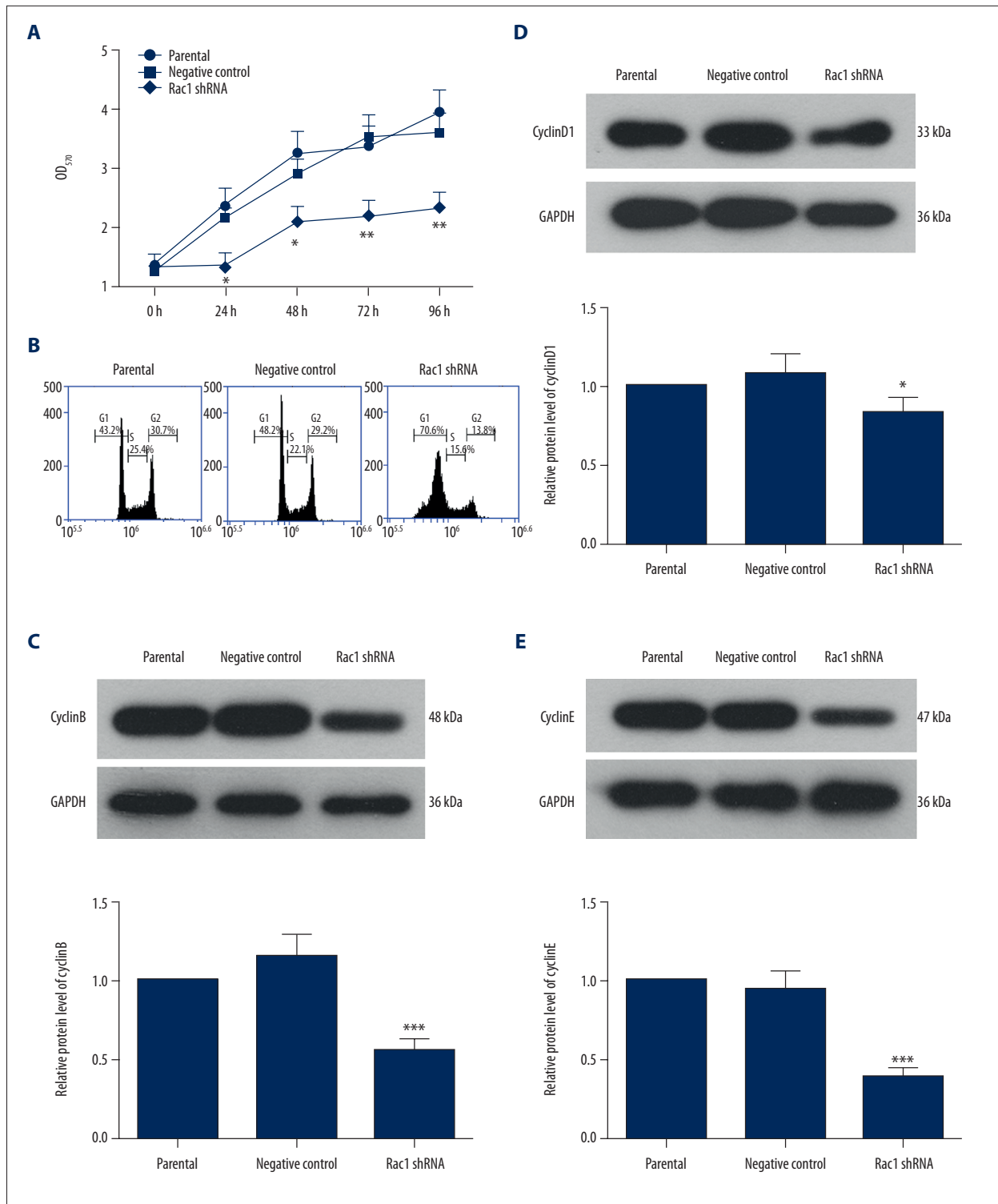


Figure 3. Rac1 shRNA inhibits the proliferation of HSCC cells and arrests their cell cycle. **(A)** The cell viability of FaDu cells was detected using MTT assay. **(B)** The cell cycle distribution of FaDu cells was detected by flow cytometry. **(C)** The protein level of cyclinB in each group was detected by Western blot analysis. GAPDH served as the internal reference. **(D)** The protein level of cyclinD1 in each group was detected by Western blot analysis using GAPDH as the internal reference. **(E)** Western blot analysis was used to detect the protein level of cyclinE in each group. Each experiment was repeated 3 times. The results are presented as mean \pm SD. * $P < 0.05$, ** $p < 0.01$, *** $p < 0.001$ compared with the negative control group.

Table 3. Ratios (%) of cells in each phase of cell cycle.

	Parental	Negative control	Rac1 shRNA
G1 phase	42.85±2.55	47.66±1.27	70.29±3.00***
S phase	25.02±2.60	23.32±2.60	15.46±2.13*
G2 phase	31.65±0.83	28.33±3.46	13.52±0.24***

* P<0.05, *** p<0.001 compared with the negative control group.

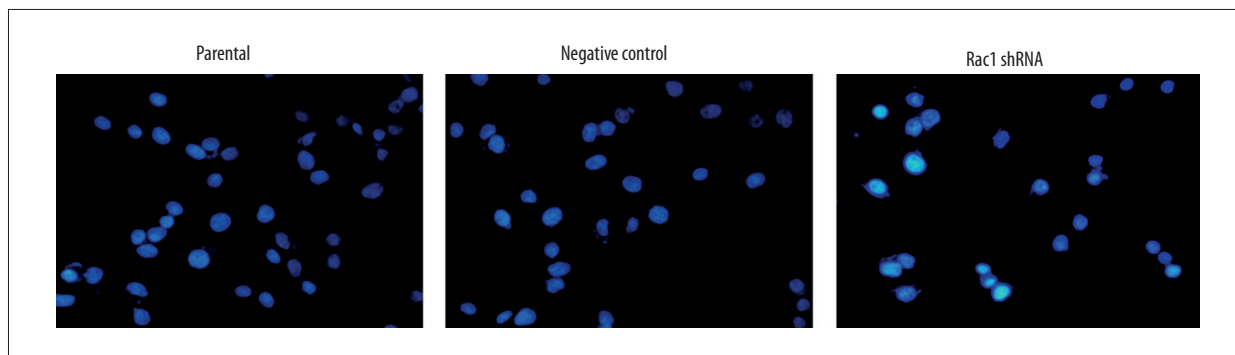
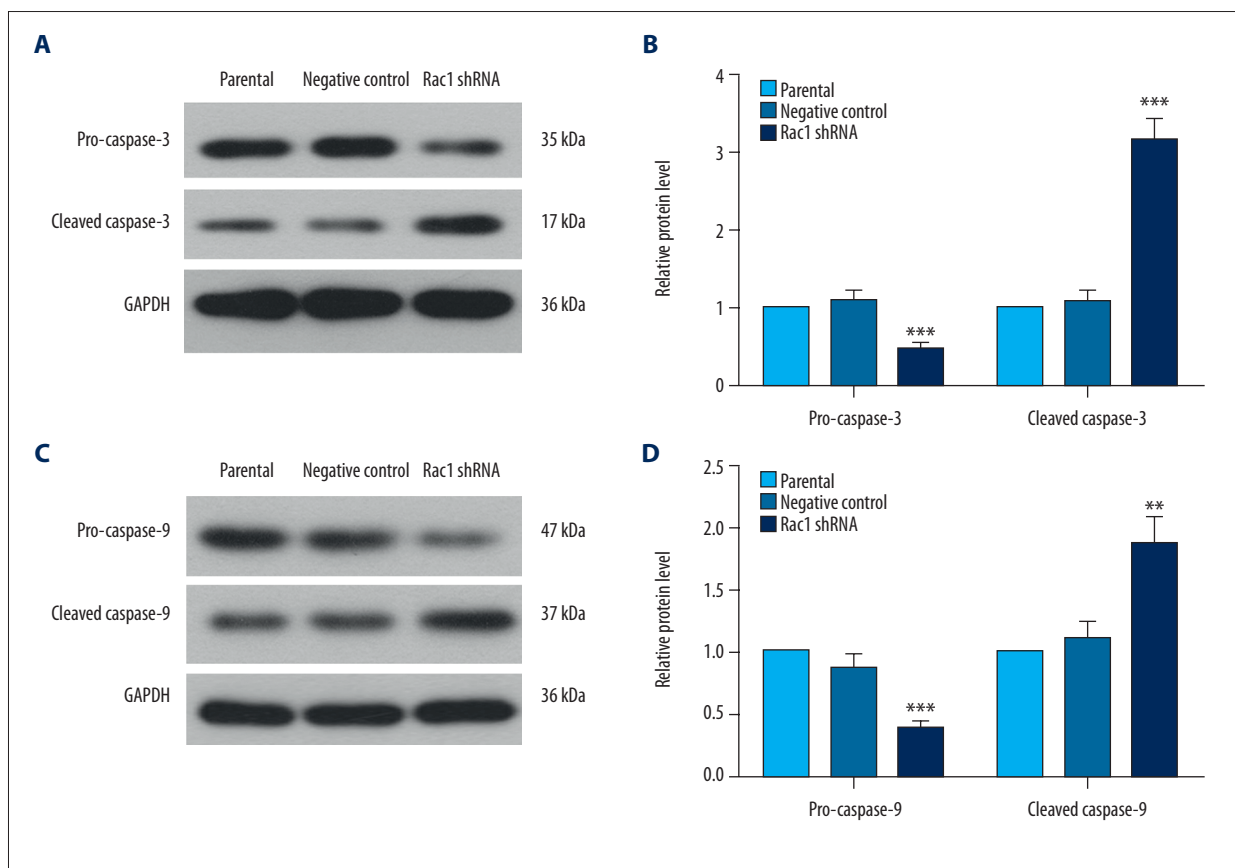


Figure 4. Rac1 silencing induces apoptosis in HSCC cells. Hoechst staining was performed to detect apoptosis in each group. All experiments were repeated 3 times.



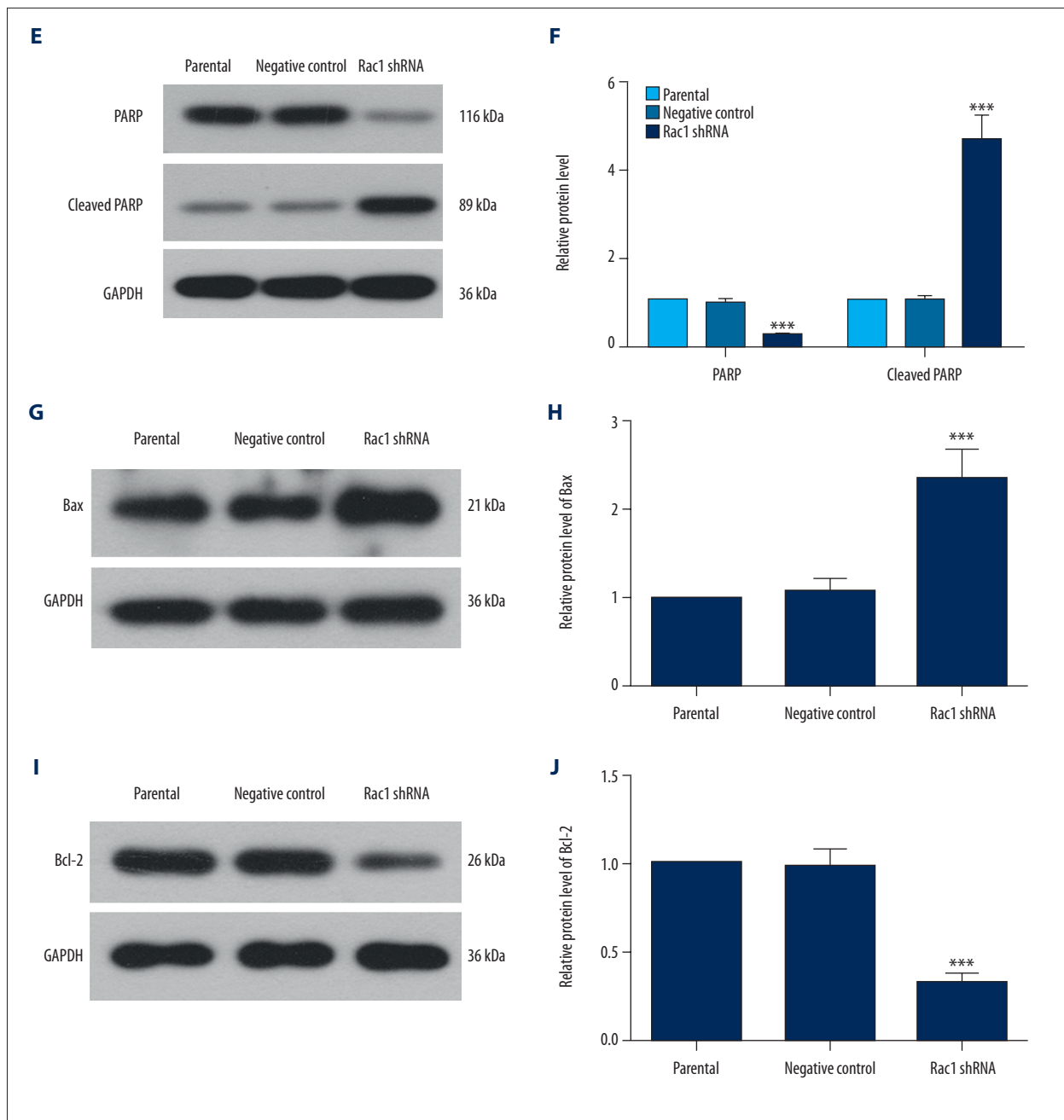


Figure 5. Silencing Rac1 affects the levels of apoptosis-related proteins. The levels of caspase-3 (A, B), caspase-9 (C, D), PARP (E, F), Bax (G, H), and Bcl-2 (I, J) were detected by Western blot analysis. The relative protein levels were calculated using GAPDH as the internal reference. All experiments were repeated 3 times and the results are presented as mean \pm SD. ** $P < 0.01$, *** $p < 0.001$ compared with the negative control group.

phosphorylation level of P38 was decreased significantly without striking changes in the protein level of P38 (Figure 8C, 8D). These results demonstrate that silencing Rac1 inhibits the activation of P38 MAPK signaling.

Silencing Rac1 inhibits the growth of HSCC *in vivo*

HSCC cells transfected with Rac1 shRNA were injected into nude mice, and then the growth of HSCC was measured. Tumor bodies in the Rac1 shRNA group showed a slower growth, with smaller tumor volumes and lower tumor weights (Figure 9A–9C). Tumor bodies in the Rac1 shRNA group also showed

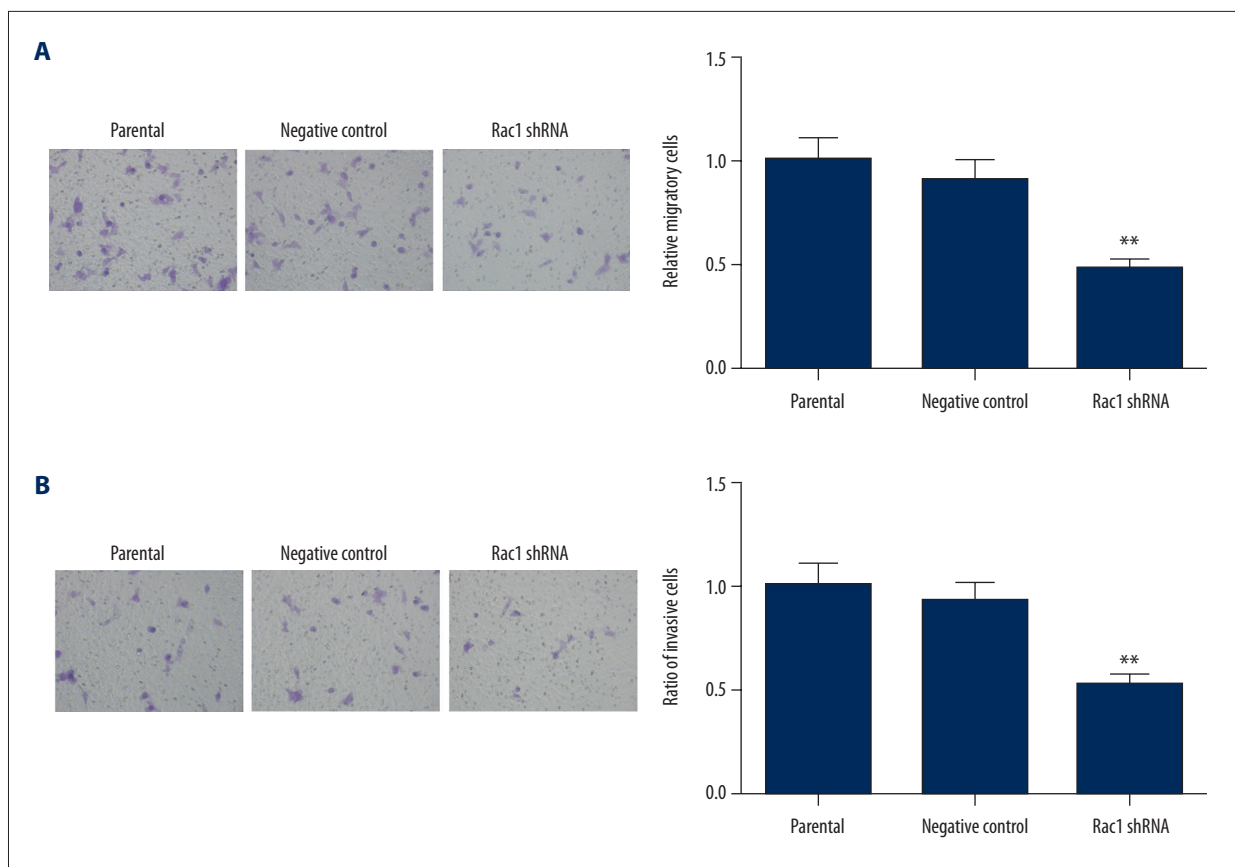


Figure 6. Rac1 silencing inhibits the migration and invasion of HSCC cells. **(A)** The migration capability of FaDu cells was assessed by Transwell assay. The ratio of migratory cells was calculated. **(B)** Transwell assay was performed to assess the invasion capability of FaDu cells. Each experiment was repeated 3 times and the results are presented as mean \pm SD. ** $P < 0.01$ compared with the negative control group.

more obvious necrotic cores (Figure 9D) and more apoptosis (Figure 9E) than in the negative control group.

As P38 MAPK signaling was inhibited by Rac1 silencing *in vitro*, the levels of MKK3 and P38 in tumor bodies were also detected. In the Rac1 shRNA group, the level of phosphorylated MKK3 was decreased significantly, with no obvious changes in MKK3 (Figure 10A, 10B). The P38 level showed no significant changes, but there was a significant decrease in phosphorylation (Figure 10C, 10D). These results demonstrate that silencing Rac1 inhibits the P38 MAPK signal *in vivo*.

Discussion

Rac1 has close relationships with cancers. In our study, the role of Rac1 in HSCC was explored *in vitro* and *in vivo*. HSCC tissues showed a higher Rac1 level. Silencing Rac1 inhibited the proliferation of HSCC cells, arrested the cell cycle, and induced apoptosis. Rac1 silencing also suppressed the migration and invasion of HSCC cells. Our *in vivo* study showed a

growth-inhibition effect of Rac1 silencing in HSCC. Moreover, *in vitro* and *in vivo* studies showed the involvement of the P38 MAPK signaling pathway in the effects of Rac1. The results of our study indicate that Rac1 has the potential to be a therapeutic target of HSCC.

Rac1 has been reported to be implicated in many diseases [15]. In the present study, HSCC tissues had high Rac1 levels, indicating that Rac1 may contribute to the pathobiology of HSCC. High Rac1 level has also been determined in many cancers, and is associated with tumor growth, metastasis, and poor prognosis [10–13,16–19].

Rac1 has close relationships with cell growth. In our study, silencing Rac1 suppressed the proliferation of HSCC cells. This indicates that Rac1 may contribute to the growth of HSCC. Rac1 downregulation was also reported to suppress the growth of osteosarcoma cells [13] and cervical cancer cells [20]. Moreover, Rac1 inhibition may enhance the sensitivity of cancer cells to radiotherapy and chemotherapy [11,21], which would benefit cancer therapy. Our study only showed data on Rac1 silencing.

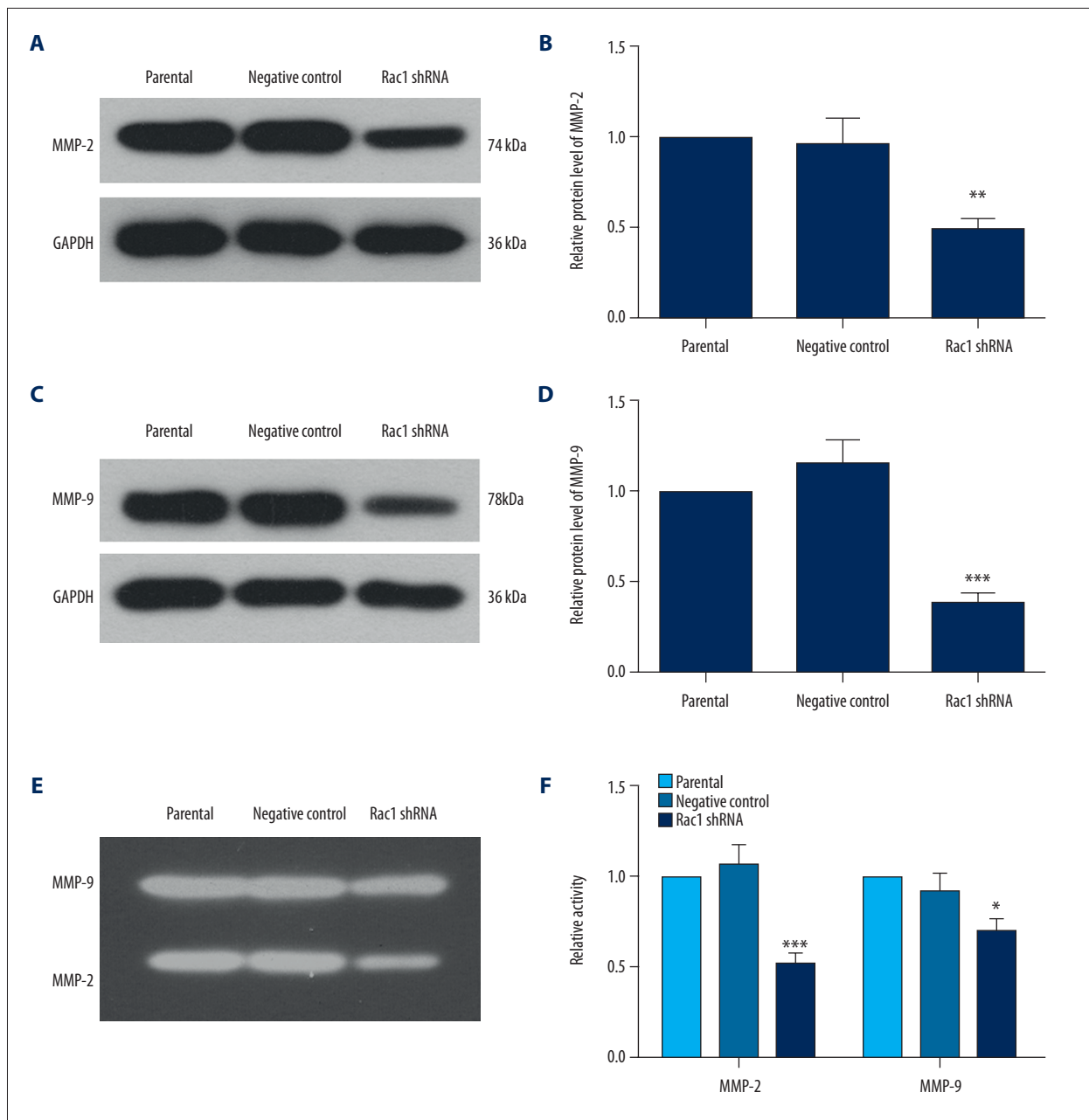


Figure 7. Rac1 shRNA inhibits the expression and activities of MMP-2 and MMP-9. Western blot analysis was performed to detect the protein levels of MMP-2 (**A, B**) and MMP-9 (**C, D**) in each group. GAPDH served as the internal reference. (**E, F**) Gelatin zymography assay was carried out to detect the activities of MMP-2 and MMP-9. All experiments were repeated 3 times and the results are presented as mean \pm SD. * $P < 0.05$, ** $p < 0.01$, *** $p < 0.001$ compared with the negative control group.

Exogenous introduction of Rac1 expression may further verify the role of Rac1 in HSCC.

Cell cycle progression is very important to cell growth. Our study showed that the cell cycle progression was arrested at G1 phase by Rac1 silencing. The report of Liu et al. also shows that the cell cycle progression of human epithelial carcinoma cells, colon cancer, and osteosarcoma is arrested at G1 phase

by Rac1 inhibition, which was consistent with our study [22]. These results indicate that Rac1 may benefit DNA synthesis and promote the cell cycle passing through the G1/S checkpoint. Moreover, Yan et al. also show that Rac1 inhibition abrogates irradiation-induced G2/M checkpoint activation, thus decreasing irradiation-induced G2/M arrest [23], which indicates that Rac1 also regulates the G2/M checkpoint. Cyclins are important regulators of the cell cycle. They are associated

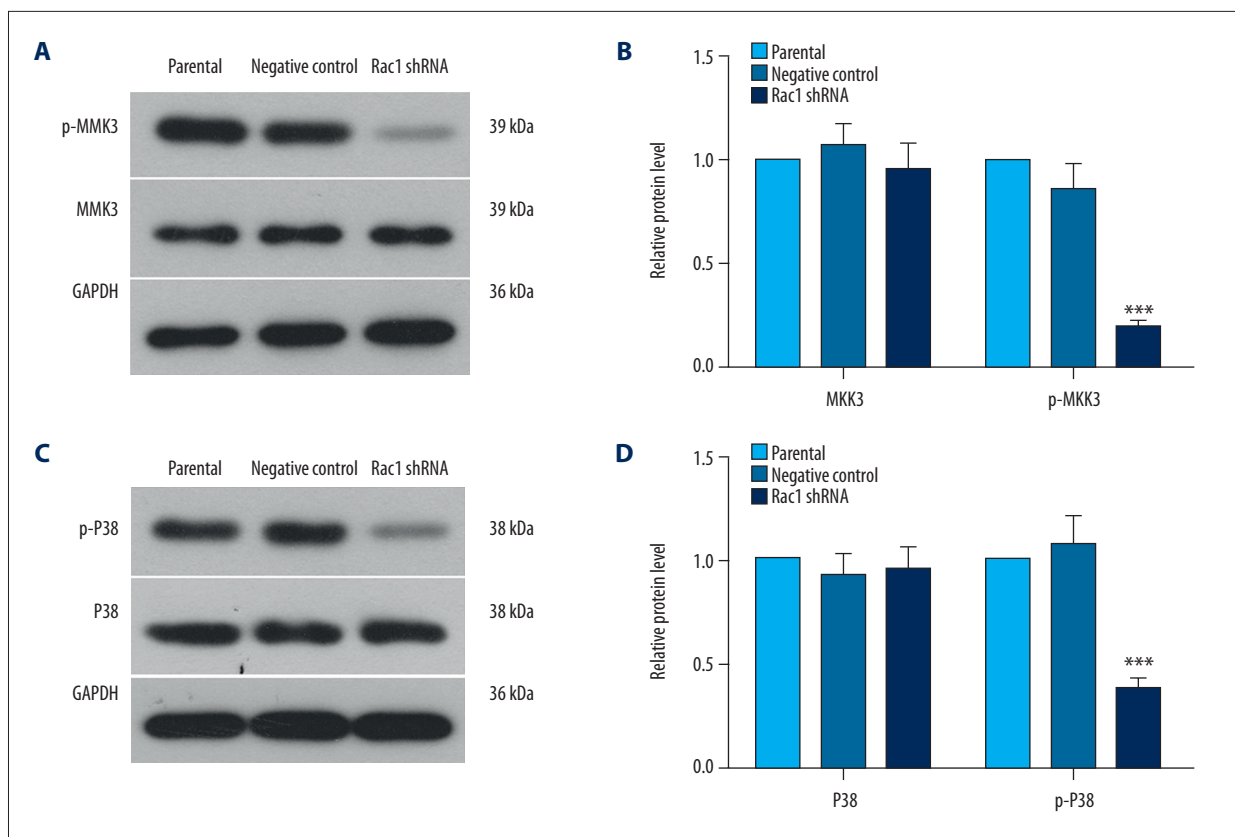


Figure 8. Silencing Rac1 inhibits the activation of P38 MAPK signal *in vitro*. The levels of MKK3 and p-MKK3 (**A, B**) and P38 and p-P38 (**C, D**) were detected by Western blot analysis. GAPDH served as the internal reference. All experiments were repeated 3 times and the results are presented as mean \pm SD. *** $P < 0.001$ compared with the negative control group.

with cyclin-dependent kinases in controlling the transition of cell cycle checkpoints. In our study, Rac1 silencing decreased the levels of cyclinB, cyclinD1, and cyclinE, which provides additional evidence for the effect of Rac1 on the cell cycle. These results suggest that Rac1 regulates cell cycle progression, thus contributing to the growth of HSCC.

Apoptosis is another important event affecting cell growth. In our study, Rac1 silencing increased the apoptosis of HSCC cells, which demonstrates that Rac1 may also perform an anti-apoptosis role in HSCC, thus contributing to the growth of HSCC. Analysis of recent studies shows that Rac1 plays complicated roles in cell apoptosis. In cancer cells, Rac1 is negatively correlated with cancer cell apoptosis [24,25]. It also protects keratinocytes from UV-induced apoptosis [26]. Rac1 is also reported to be requisite for cardiomyocyte apoptosis during hyperglycemia [27]. The causes of these different roles of Rac1 in apoptosis remain unclear and need further exploration.

Rac1 silencing inhibited the proliferation, arrested the cell cycle, and induced apoptosis in HSCC cells, demonstrating a growth-inhibition role of Rac1 silencing in HSCC cells. Our *in vivo* study also showed a growth-inhibition effect of Rac1 silencing on

HSCC. Consistent with our results, Bopp et al. showed that lack of Rac1 reduces diethylnitrosamine-induced liver cancer [28]. Compounds that inhibit Rac1 are also reported to show significant growth-inhibition effects in cancers [29,30]. Therefore, Rac1 has the potential to be a therapeutic target for HSCC. In addition, Rac1 also affects tumor angiogenesis, which is beneficial to nutritional supplementation and cancer metastasis [14]. Moreover, inhibition of Rac1 is reported to strengthen the sensitivity of cancer cells to radiotherapy and chemotherapy [11,23,31,32]. Thus, therapy targeting Rac1 may have excellent efficacy. However, as Rac1 is ubiquitously expressed throughout the body, targeted delivery systems need further development to avoid adverse effects.

Metastasis is a main cause of mortality in cancer patients. An estimated 90% of cancer-associated deaths are caused by metastasis [33]. Rac1 can regulate cytoskeleton reorganization, promote the formation of lamellipodia, and is associated with the metastasis of many cancers [5,14,34–37]. In our study, silencing Rac1 inhibited the migration and invasion of HSCC cells, indicating that Rac1 may also contribute to HSCC metastasis. MMPs play important roles in extracellular matrix degradation, which contributes to the metastasis of cancer

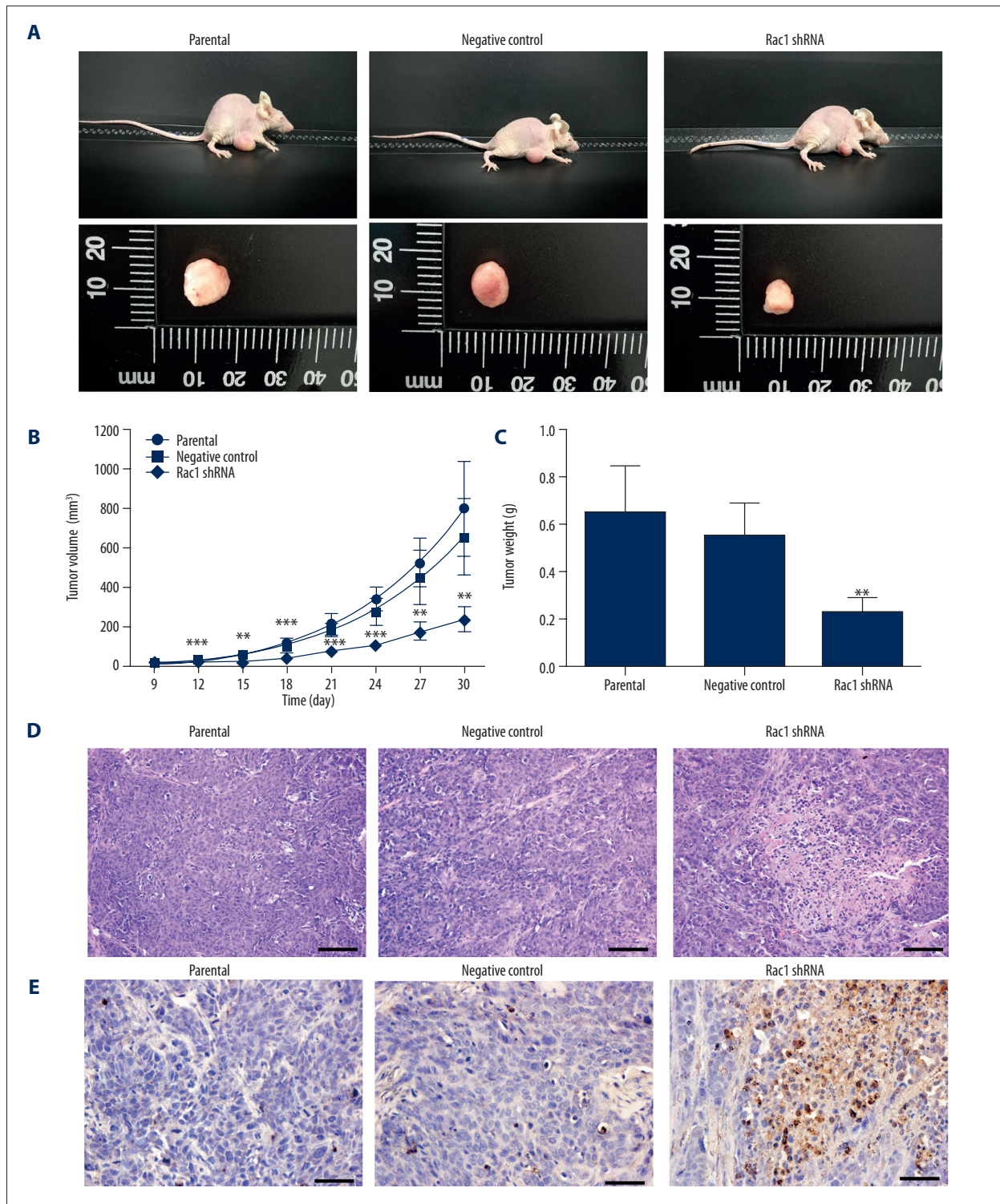


Figure 9. Rac1 shRNA inhibits the growth of HSCC cells *in vivo*. (A) Mice in each group were inoculated with parental cells, Rac1 shRNA cells, or negative control cells. Thirty days after inoculation, the mice were killed and the tumor bodies were obtained. (B) The volumes of tumor bodies were measured every 3 days. (C) The weights of tumor bodies in each group. (D) HE staining was carried out to assess the histopathologic changes in each group. Scale bar=100 μ m. (E) TUNEL assay was performed to detect apoptosis in each group. Scale bar=50 μ m. Typical results are presented. N=6. The results are presented as mean \pm SD. ** $P < 0.01$, *** $p < 0.001$ compared with the negative control group.

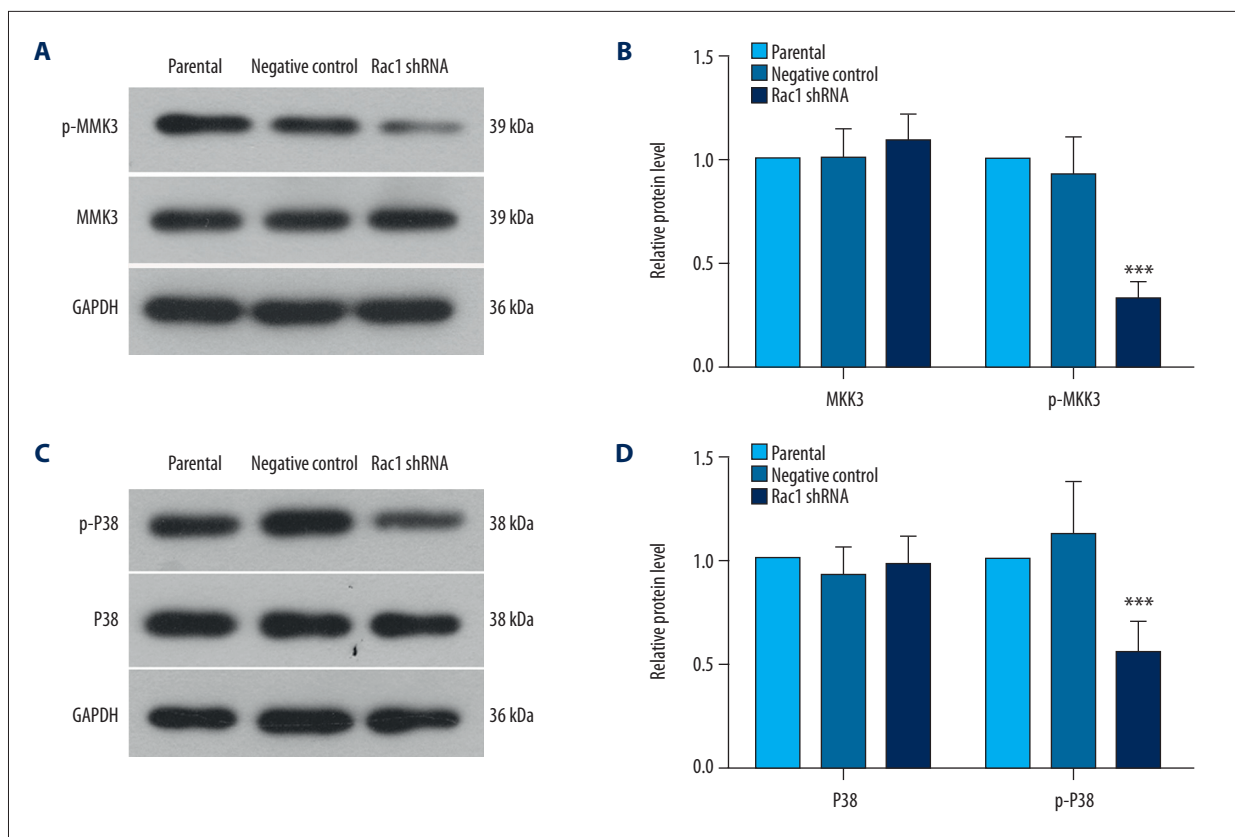


Figure 10. Rac1 silencing inhibits the activation of P38 MAPK signal *in vivo*. The levels of MKK3 and p-MKK3 (A, B) and P38 and p-P38 (C, D) in each group were detected by Western blot analysis with GAPDH as the internal reference. All experiments were repeated 3 times. The results are presented as mean \pm SD. N=6. *** P<0.001 compared with the negative control group.

cells [38,39]. In our study, the expression and activities of MMP-2 and MMP-9 were all decreased by Rac1 silencing. These results provide additional evidence for the metastasis-inhibition effect of Rac1 silencing in HSCC cells. Rac1 is also reported to be involved in the epithelial-mesenchymal transition, which is one of the important events in cancer cell metastasis [40]. As a limitation of our study, we lacked experiments regarding tumor metastasis *in vivo*. Although Lee et al. showed that inhibition of Rac1 can decrease tumor metastasis *in vivo* [41], the effect of Rac1 silencing on the *in vivo* metastasis of HSCC needs further exploration.

Rac1 interacts directly with several signals to regulate cell growth, inflammatory responses, and cell-cell contacts [14]. MAPK family members can be activated by Rac1. P38 MAPK signalling is implicated in diverse cellular events through its extensive downstream molecules [42]. In our study, the activation of P38 MAPK signalling was inhibited by Rac1 silencing, both *in vivo* and *in vitro*. These results suggest that Rac1 affects the

growth and metastasis of HSCC through P38 MAPK signalling. Other signals, such as Wnt [43], are also downstream of Rac1, and they may also be involved in the role of Rac1 in HSCC, but further explorations are needed to assess this.

Conclusions

In our study, Rac1 showed a high level in HSCC tissues. Silencing Rac1 inhibited the growth of HSCC *in vitro* and *in vivo*. Rac1 silencing was also found to suppress the metastasis of HSCC cells. This indicates that Rac1 may act as an oncogene in HSCC and has the potential to become a promising therapeutic target for HSCC.

Conflict of interest

None.

References:

1. Takes RP, Strojan P, Silver CE et al: Current trends in initial management of hypopharyngeal cancer: the declining use of open surgery. *Head Neck*, 2012; 34: 270–81
2. Hall SF, Groome PA, Irish J, O'Sullivan B: The natural history of patients with squamous cell carcinoma of the hypopharynx. *Laryngoscope*, 2008; 118: 1362–71
3. Harris BN, Biron VL, Donald P et al: Primary surgery vs. chemoradiation treatment of advanced-stage hypopharyngeal squamous cell carcinoma. *JAMA Otolaryngol Head Neck Surg*, 2015; 141: 636–40
4. Wycliffe ND, Grover RS, Kim PD, Simental A Jr.: Hypopharyngeal cancer. *Top Magn Reson Imaging*, 2007; 18: 243–58
5. Wertheimer E, Gutierrez-Uzquiza A, Roseblit C et al: Rac signaling in breast cancer: a tale of GEFs and GAPs. *Cell Signal*, 2012; 24: 353–62
6. Bosco EE, Mulloy JC, Zheng Y: Rac1 GTPase: a "Rac" of all trades. *Cell Mol Life Sci*, 2009; 66: 370–74
7. Hall A: Rho GTPases and the control of cell behaviour. *Biochem Soc Trans*, 2005; 33: 891–95
8. Gastonguay A, Berg T, Hauser AD et al: The role of Rac1 in the regulation of NF-kappaB activity, cell proliferation, and cell migration in non-small cell lung carcinoma. *Cancer Biol Ther*, 2012; 13: 647–56
9. Michaelson D, Abidi W, Guardavaccaro D et al: Rac1 accumulates in the nucleus during the G2 phase of the cell cycle and promotes cell division. *J Cell Biol*, 2008; 181: 485–96
10. Hein AL, Post CM, Sheinin YM et al: RAC1 GTPase promotes the survival of breast cancer cells in response to hyper-fractionated radiation treatment. *Oncogene*, 2016; 35: 6319–29
11. Yan Y, Hein AL, Etekpo A et al: Inhibition of RAC1 GTPase sensitizes pancreatic cancer cells to gamma-irradiation. *Oncotarget*, 2014; 5: 10251–70
12. Ji J, Feng X, Shi M et al: Rac1 is correlated with aggressiveness and a potential therapeutic target for gastric cancer. *Int J Oncol*, 2015; 46: 1343–53
13. Zheng Z, Ding M, Ni J et al: MiR-142 acts as a tumor suppressor in osteosarcoma cell lines by targeting Rac1. *Oncol Rep*, 2015; 33: 1291–99
14. Bid HK, Roberts RD, Manchanda PK, Houghton PJ: RAC1: An emerging therapeutic option for targeting cancer angiogenesis and metastasis. *Mol Cancer Ther*, 2013; 12: 1925–34
15. Marei H, Malliri A: Rac1 in human diseases: The therapeutic potential of targeting Rac1 signaling regulatory mechanisms. *Small GTPases*, 2017; 8(3): 139–63
16. Liu B, Xiong J, Liu G et al: High expression of Rac1 is correlated with partial reversed cell polarity and poor prognosis in invasive ductal carcinoma of the breast. *Tumour Biol*, 2017; 39: 1010428317710908
17. Chen QY, Xu LQ, Jiao DM et al: Silencing of Rac1 modifies lung cancer cell migration, invasion and actin cytoskeleton rearrangements and enhances chemosensitivity to antitumor drugs. *Int J Mol Med*, 2011; 28: 769–76
18. Yuan K, Qian C, Zheng R: Prognostic significance of immunohistochemical Rac1 expression in survival in early operable non-small cell lung cancer. *Med Sci Monit*, 2009; 15: BR313–19
19. Kamai T, Yamanishi T, Shirataki H et al: Overexpression of RhoA, Rac1, and Cdc42 GTPases is associated with progression in testicular cancer. *Clin Cancer Res*, 2004; 10: 4799–805
20. Xu AL, Yu GQ, Kong XC et al: Effect of Rac1 downregulation mediated by shRNA on the biological behaviour of human cervical cancer cells. *J Int Med Res*, 2013; 41: 1037–48
21. Kaneto N, Yokoyama S, Hayakawa Y et al: RAC1 inhibition as a therapeutic target for gefitinib-resistant non-small-cell lung cancer. *Cancer Sci*, 2014; 105: 788–94
22. Liu L, Zhang H, Shi L et al: Inhibition of Rac1 activity induces G1/S phase arrest through the GSK3/cyclin D1 pathway in human cancer cells. *Oncol Rep*, 2014; 32: 1395–400
23. Yan Y, Greer PM, Cao PT et al: RAC1 GTPase plays an important role in gamma-irradiation induced G2/M checkpoint activation. *Breast Cancer Res*, 2012; 14: R60
24. Yoshida T, Zhang Y, Rivera Rosado LA et al: Blockade of Rac1 activity induces G1 cell cycle arrest or apoptosis in breast cancer cells through downregulation of cyclin D1, survivin, and X-linked inhibitor of apoptosis protein. *Mol Cancer Ther*, 2010; 9: 1657–68
25. Faria M, Matos P, Pereira T et al: RAC1b overexpression stimulates proliferation and NF-kB-mediated anti-apoptotic signaling in thyroid cancer cells. *PLoS One*, 2017; 12: e0172689
26. Deshmukh J, Pofahl R, Haase I: Epidermal Rac1 regulates the DNA damage response and protects from UV-light-induced keratinocyte apoptosis and skin carcinogenesis. *Cell Death Dis*, 2017; 8: e2664
27. Shen E, Li Y, Shan L et al: Rac1 is required for cardiomyocyte apoptosis during hyperglycemia. *Diabetes*, 2009; 58: 2386–95
28. Bopp A, Wartlick F, Henninger C et al: Rac1 promotes diethylnitrosamine (DEN)-induced formation of liver tumors. *Carcinogenesis*, 2015; 36: 378–89
29. Castillo-Pichardo L, Humphries-Bickley T, De La Parra C et al: The Rac inhibitor EHop-016 inhibits mammary tumor growth and metastasis in a nude mouse model. *Transl Oncol*, 2014; 7: 546–55
30. Zins K, Lucas T, Reichl P et al: A Rac1/Cdc42 GTPase-specific small molecule inhibitor suppresses growth of primary human prostate cancer xenografts and prolongs survival in mice. *PLoS One*, 2013; 8: e74924
31. Wang JY, Yu P, Chen S et al: Activation of Rac1 GTPase promotes leukemia cell chemotherapy resistance, quiescence and niche interaction. *Mol Oncol*, 2013; 7: 907–16
32. Skvortsov S, Dudas J, Eichberger P et al: Rac1 as a potential therapeutic target for chemo-radioresistant head and neck squamous cell carcinomas (HNSCC). *Br J Cancer*, 2014; 110: 2677–87
33. Mehlen P, Puisieux A: Metastasis: A question of life or death. *Nat Rev Cancer*, 2006; 6: 449–58
34. Wu YI, Frey D, Lungu OI et al: A genetically encoded photoactivatable Rac controls the motility of living cells. *Nature*, 2009; 461: 104–8
35. Sanz-Moreno V, Gadea G, Ahn J et al: Rac activation and inactivation control plasticity of tumor cell movement. *Cell*, 2008; 135: 510–23
36. Parri M, Chiarugi P: Rac and Rho GTPases in cancer cell motility control. *Cell Commun Signal*, 2010; 8: 23
37. Arnold CR, Abdelmoez A, Thurner G et al: Rac1 as a multifunctional therapeutic target to prevent and combat cancer metastasis. *Oncoscience*, 2014; 1: 513–21
38. Stetler-Stevenson WG, Yu AE: Proteases in invasion: Matrix metalloproteinases. *Semin Cancer Biol*, 2001; 11: 143–52
39. Webb AH, Gao BT, Goldsmith ZK et al: Inhibition of MMP-2 and MMP-9 decreases cellular migration, and angiogenesis in *in vitro* models of retinoblastoma. *BMC Cancer*, 2017; 17: 434
40. Lv Z, Hu M, Zhen J et al: Rac1/PAK1 signaling promotes epithelial-mesenchymal transition of podocytes *in vitro* via triggering beta-catenin transcriptional activity under high glucose conditions. *Int J Biochem Cell Biol*, 2013; 45: 255–64
41. Lee JW, Ryu YK, Ji YH et al: Hypoxia/reoxygenation-experienced cancer cell migration and metastasis are regulated by Rap1- and Rac1-GTPase activation via the expression of thymosin beta-4. *Oncotarget*, 2015; 6: 9820–33
42. Ono K, Han J: The p38 signal transduction pathway: Activation and function. *Cell Signal*, 2000; 12: 1–13
43. Jamieson C, Lui C, Brocardo MG et al: Rac1 augments Wnt signaling by stimulating beta-catenin-lymphoid enhancer factor-1 complex assembly independent of beta-catenin nuclear import. *J Cell Sci*, 2015; 128: 3933–46